

New constraints on R-parity violating couplings through the measurements of the $B_{s(d)}^0$ - $\bar{B}_{s(d)}^0$ and K^0 - \bar{K}^0 mixing

Gao Xiangdong,^{*} Chong Sheng Li,[†] and Li Lin Yang[‡]

Department of Physics, Peking University, Beijing 100871, China

(Dated: June 20, 2021)

Abstract

We calculate contributions to $B_s - \bar{B}_s$ mixing through tree-level sneutrino exchange in the framework of the minimal supersymmetric standard model with R-parity violation, including the next-to-leading-order QCD corrections. We compare our results with the updated bounds on the $B_s - \bar{B}_s$ mass difference reported by CDF collaborations, and present new constraints on the relevant combinations of parameters of the minimal supersymmetric standard model with R-parity violation. Our results show that upper bound on the relevant combination of couplings of $B_s - \bar{B}_s$ mixing is of the order 10^{-9} . We also calculate the $B_d^0 - \bar{B}_d^0$ and $K^0 - \bar{K}^0$ mass differences, and show that the upper bounds on the relevant combinations of couplings are two and four orders of magnitude stronger than ones reported in the literatures, respectively. We also discuss the case of complex couplings and show that how the relevant combinations of couplings are constrained by the updated experiment data of $B_s - \bar{B}_s$, $B_d - \bar{B}_d$ mixing and time-dependent CP asymmetry $S_{J/\psi K_s}$, and future possible observations of $S_{J/\psi\phi}$ at LHCb, respectively.

PACS numbers: 14.40.Nd, 12.60.Jv, 12.15.Mm, 14.80.Ly

^{*}Electronic address: gaoxiangdong@pku.edu.cn

[†]Electronic address: cshi@pku.edu.cn

[‡]Electronic address: llyang@pku.edu.cn

I. INTRODUCTION

Very recently, the DØ collaboration and the CDF collaboration at the Fermilab Tevatron reported their updated measurements of the mass difference between B_s and \bar{B}_s mesons (Δm_s). The new bounds on the mass difference are [1, 2]:

$$\begin{aligned} \text{DØ: } & 17 \text{ ps}^{-1} < \Delta m_s < 21 \text{ ps}^{-1} \\ \text{CDF: } & \Delta m_s = 17.77_{-0.10}^{+0.10} \pm 0.07 \text{ ps}^{-1} \end{aligned} \quad (1)$$

It was the first time that both the lower bound and the upper bound for the $B_s - \bar{B}_s$ mixing are presented. Especially the CDF result has reached an accuracy of about 1%. The new results are important for the precision test of the standard model (SM), especially for the determination of the unitary triangle. Moreover, if the SM predictions are consistent with the above results, these data will put severe constraints on the flavor structure of the possible new physics models beyond the SM.

In the literature, there have already been many discussions about the implications of the new measurements. In Ref. [3, 4, 5, 6, 7], the authors carried out model-independent analysis of the constraints on extensions of the SM. There are also model-dependent calculations in some new physics models beyond the SM [8, 9, 10, 11, 12, 13, 14]. In this paper, we further investigate the effects of the minimal supersymmetric standard model with R-parity violation (MSSM-RPV) [15] on the neutral meson mixing.

R-parity is a discrete symmetry defined by $R_p = (-1)^{3B+L+2S}$, where B is the baryon number, L is the lepton number and S is the spin of the particle. In a supersymmetric extension of the SM, all the particles in the SM have $R_p = 1$, while all the superpartners have $R_p = -1$. R-parity conservation is imposed in the minimal supersymmetric standard model (MSSM) to keep proton stable. However, this requirement is not necessary for a fundamental theory, and one can always introduce lepton number or baryon number violating terms in the Lagrangian. For the neutral meson mixing, the relevant terms in the Lagrangian are

$$\mathcal{L}_{\text{RPV}} = \lambda'_{ijk} \tilde{\nu}_{iL} \bar{d}_{kR} d_{jL} + h.c. \quad (2)$$

These interaction terms can induce $B_s - \bar{B}_s$ mixing through tree level sneutrino exchange, and thus, probably, the relevant combination of couplings $\sum_i \lambda'_{i32} \lambda'^*_{i23}$ will be severely constrained by the recent measurements [1, 2]. Similarly, the terms shown in Eq. (2) also can induce

the $B_d^0 - \bar{B}_d^0$ and $K^0 - \bar{K}^0$ mixing, which were discussed in Ref. [16] at the leading-order, and the constraints on the relevant combinations of couplings through comparing with data were given by [16]

$$\begin{aligned}\sum_i \lambda'_{i31} \lambda'^*_{i13} n_i &\lesssim 3.3 \times 10^{-8}, \\ \sum_i \lambda'_{i21} \lambda'^*_{i12} n_i &\lesssim 4.5 \times 10^{-9},\end{aligned}\tag{3}$$

where $n_i \equiv (100 \text{ GeV}/m_{\tilde{\nu}_{iL}})^2$, $m_{\tilde{\nu}_{iL}}$ is the mass of the sneutrino of the i -th generation. However, authors of Ref. [16] did not include the contributions of the SM, since they believed that both theoretical and experimental results involved considerable uncertainties at that time. Recently, both SM theoretical predictions and experimental results has been improved significantly [17]. Thus, besides investigating of B_s^0 - \bar{B}_s^0 mixing, it is also worthwhile to reinvestigate the constraints on the combinations of R-parity violating (RPV) couplings with the updated data on B_d^0 - \bar{B}_d^0 and K^0 - \bar{K}^0 mixing including the SM contributions. Moreover, in general, the next-to-leading-order (NLO) QCD corrections are significant, so we also calculate the NLO QCD effects on the above neutral meson mixing in this paper.

In addition to the above mass differences, the R-parity violating couplings can also contribute to the CP asymmetries in the meson decay processes, when the couplings are complex. So the combinations of RPV couplings discussed above can affect observables related to time-dependent CP violation in processes such as $B_d \rightarrow J/\psi K_s$ and $B_s \rightarrow J/\psi \phi$. In this paper, we also consider the constraints on the relevant combinations of MSSM-RPV couplings from these CP violation observables.

We organize our paper as following. Section II is a brief summary of the formalism for the calculation of the neutral meson mixing, CP asymmetry in B physics and the results in the SM. In Section III, we calculate the contributions from the MSSM-RPV at leading-order and next-to-leading-order in QCD. In section IV, we present our numerical results and discussions.

II. BASIC FORMALISM AND ANALYTICAL RESULTS IN THE SM

In order to make our paper self-contained, we first illustrate the basic formalism for the calculation of the $B_{s(d)}^0$ - $\bar{B}_{s(d)}^0$ and K^0 - \bar{K}^0 mass differences Δm , the time-dependent CP asymmetry in B_d decay, $S_{J/\psi K_s}$ and the time-dependent CP asymmetry in B_s decay, $S_{J/\psi \phi}$.

We start from the $\Delta F = 2$ effective Hamiltonian [18]

$$\mathcal{H}_{\text{eff}} = \sum_i C_i Q_i + h.c.. \quad (4)$$

The relevant operators for our concerning are

$$Q_0 = \bar{q}^\alpha \gamma_\mu P_L b^\alpha \bar{q}^\beta \gamma_\mu P_L b^\beta, \quad (5)$$

$$Q_1 = \bar{q}^\alpha P_L b^\alpha \bar{q}^\beta P_R b^\beta, \quad (6)$$

$$Q_2 = \bar{q}^\alpha P_L b^\beta \bar{q}^\beta P_R b^\alpha, \quad (7)$$

where $q = d, s$ for B_d or B_s meson mixing, respectively. Similar expressions for $K^0 - \bar{K}^0$ mixing can be obtained by replacing b with s and setting $q = d$.

With this effective Hamiltonian, the $B_q - \bar{B}_q$ mass difference can be expressed as

$$\Delta m_q = 2 \left| \langle \bar{B}_q | \mathcal{H}_{\text{eff}} | B_q \rangle \right| = 2 \left| \sum_i C_i \langle \bar{B}_q | Q_i | B_q \rangle \right|; \quad (8)$$

$a_{J/\psi K_s(\phi)}$, time-dependent CP asymmetry in $B_{d(s)} \rightarrow J/\psi K_s(\phi)$ decays, can be expressed as

$$a_{J/\psi K_s(\phi)} = S_{J/\psi K_s(\phi)} \sin \Delta m_{d(s)} t, \quad (9)$$

where $S_{J/\psi K_s(\phi)} = \sin 2\beta_{eff}$, and $\beta_{eff} = \frac{1}{2} \arg \langle \bar{B}_{d(s)} | \mathcal{H}_{\text{eff}} | B_{d(s)} \rangle$. In the framework of SM,

$$S_{J/\psi K_s}^{SM} = \sin 2\beta, \quad S_{J/\psi \phi}^{SM} = \sin 2\beta_s, \quad (10)$$

with

$$\begin{aligned} \beta &= \arg \left(-\frac{(V_{CKM})_{cd}(V_{CKM}^*)_{cb}}{(V_{CKM})_{td}(V_{CKM}^*)_{tb}} \right), \\ \beta_s &= \arg \left(-\frac{(V_{CKM})_{ts}(V_{CKM}^*)_{tb}}{(V_{CKM})_{cs}(V_{CKM}^*)_{cb}} \right). \end{aligned} \quad (11)$$

In the SM, only C_0 is nonzero, which has been calculated to the NLO in QCD [18, 19] and is given by

$$C_0(\mu) = \frac{G_F^2 m_W^2}{4\pi^2} (V_{tb}^* V_{tq})^2 \eta_B S_0(x_t) \left(\alpha_s^{(5)}(\mu) \right)^{-6/23} \left[1 + \frac{\alpha_s^{(5)}(\mu)}{4\pi} J_5 \right], \quad (12)$$

where $\eta_B = 0.55 \pm 0.1$ [20], $J_5 = 1.627$ in the naive dimensional regularization scheme (NDR), $x_t = m_t^2/m_W^2$ and $S_0(x_t)$ is the Inami-Lim function [21]. The scale μ is usually taken to be $\sim m_b$ in B physics.

	$B_0(\mu)$	$B_1(\mu)$	$B_2(\mu)$
$K^0(\mu = 2GeV)$	0.69	1.03	0.73
$B_d(\mu = m_b)$	0.87	1.16	1.91
$B_s(\mu = m_b)$	0.86	1.17	1.94

TABLE I: Non-perturbative parameters used in our numerical calculations.

The expression for the $K^0 - \bar{K}^0$ mass difference is a little different, which is given by

$$\Delta m_K = 2\text{Re} \langle \bar{K}^0 | \mathcal{H}_{\text{eff}} | K^0 \rangle = 2\text{Re} \sum_i C_i \langle \bar{K}^0 | Q_i | K^0 \rangle. \quad (13)$$

The nonzero NLO Wilson coefficient in the SM is

$$C_0(\mu) = \frac{G_F^2 m_W^2}{4\pi^2} [\lambda_c^2 \eta_1 S_0(x_c) + \lambda_t^2 \eta_2 S_0(x_t) + 2\lambda_c \lambda_t \eta_3 S_0(x_c, x_t)] (\alpha_s^{(3)}(\mu))^{-2/9} \left[1 + \frac{\alpha_s^{(3)}(\mu)}{4\pi} J_3 \right], \quad (14)$$

where $\lambda_i = V_{is}^* V_{id}$, $J_3 = 1.895$ in the NDR scheme and the parameters η_i are $\eta_1 = 1.38 \pm 0.20$, $\eta_2 = 0.57 \pm 0.01$, $\eta_3 = 0.47 \pm 0.04$ [20, 22], respectively. S_0 functions can be found in Ref.[18].

The matrix elements of the operators Q_i ($i=0,1,2$) between two hadronic states can be obtained by using the vacuum insertion approximation (VIA) and partial axial current conservation (PCAC). We refer the readers to Ref. [23] for details. The results are

$$\langle Q_0(\mu) \rangle \equiv \langle \bar{B}_s | Q_0(\mu) | B_s \rangle = \frac{1}{3} f_{B_s}^2 m_{B_s} B_0(\mu), \quad (15)$$

$$\langle Q_1(\mu) \rangle \equiv \langle \bar{B}_s | Q_1(\mu) | B_s \rangle = f_{B_s}^2 m_{B_s} \left(\frac{1}{24} - \frac{m_{B_s}^2}{4(m_s(\mu) + m_b(\mu))^2} \right) B_1(\mu), \quad (16)$$

$$\langle Q_2(\mu) \rangle \equiv \langle \bar{B}_s | Q_2(\mu) | B_s \rangle = f_{B_s}^2 m_{B_s} \left(\frac{1}{8} - \frac{m_{B_s}^2}{12(m_s(\mu) + m_b(\mu))^2} \right) B_2(\mu), \quad (17)$$

where m_{B_s} and f_{B_s} is the mass and decay constant of the B_s mesons, respectively. Clearly, the expressions for B_d and K^0 mesons can be obtained by simple substitutions. $B_i(\mu)$ is the non-perturbative parameters and can be calculated with lattice method [24, 25]. We list their values to be used in our numerical calculations in table I:

III. MSSM-RPV CONTRIBUTIONS AND NLO QCD CORRECTIONS

In the MSSM-RPV, there are tree-level contributions to the $B_{s(d)} - \bar{B}_{s(d)}$ and $K^0 - \bar{K}^0$ mixing through sneutrino exchange. The tree diagrams contribute through the operator Q_1 ,

and the corresponding Wilson coefficient is

$$C_1 = - \sum_i \frac{\lambda'_{ijk} \lambda_{ikj}^*}{m_{\tilde{\nu}_i}^2} + \mathcal{O}(\alpha_s), \quad (18)$$

where $jk = 32, 31, 21$ for B_s, B_d and K^0 mesons, respectively. We assume universal sneutrino masses for simplicity, i.e., $m_{\tilde{\nu}_i} = m_{\tilde{\nu}}, i = 1, 2, 3$.

At NLO in QCD, both Q_1 and Q_2 contribute due to color exchange. To calculate the NLO Wilson coefficients, we match the full theory onto the effective theory at the SUSY scale, and then run the coefficients down to the hadronic scales using the renormalization group equations (RGE). In our calculations, we use dimensional regularization in $d = 4 - 2\epsilon$ dimensions to regulate, and use $\overline{\text{MS}}$ scheme to renormalize the ultraviolet (UV) divergences. We keep the heaviest quark mass m_Q ($Q = b$ for B mesons and $Q = s$ for K mesons) and set all other quark masses to be zero in the Wilson coefficients. However, we will keep the lighter quark mass m_q in the intermediate stages of our calculation in order to regulate the infrared (IR) divergences. We also set all external momenta to zero, since the coefficients should not depend on them.

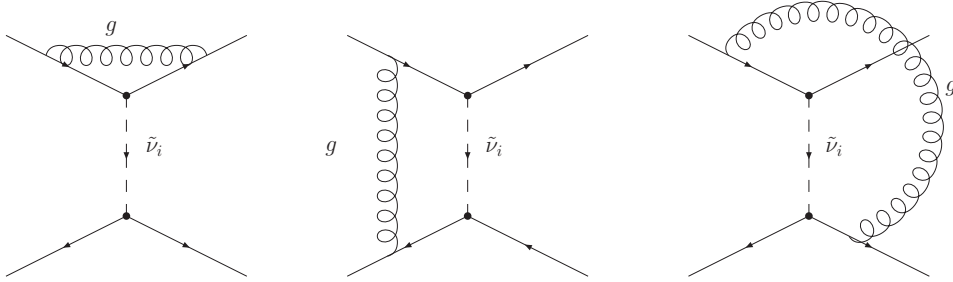


FIG. 1: One-loop Feynman diagrams in the full theory.

The NLO diagrams in the full theory are shown in Fig. 1. In the full theory, all the UV divergences should be removed by the renormalization of the quark wave functions and the coupling constants. The renormalized amplitude in the full theory is

$$A_{\text{full}} = - \sum_i \frac{\lambda'_{ijk} \lambda_{ikj}^*}{m_{\tilde{\nu}}^2} \left\{ \left[1 + \frac{\alpha_s}{\pi} C_F \left(1 - 2 \ln \frac{m_Q^2}{\mu^2} \right) + \frac{\alpha_s}{4\pi} \frac{m_{\tilde{\nu}}^2 \ln \frac{m_Q^2}{m_q^2} + m_Q^2 \ln \frac{m_q^2}{m_{\tilde{\nu}}^2}}{m_{\tilde{\nu}}^2 - m_Q^2} \right] \langle Q_1 \rangle_{\text{tree}} - \frac{\alpha_s}{4\pi} \frac{1}{N} \frac{m_{\tilde{\nu}}^2 \ln \frac{m_Q^2}{m_q^2} + m_Q^2 \ln \frac{m_q^2}{m_{\tilde{\nu}}^2}}{m_{\tilde{\nu}}^2 - m_Q^2} \langle Q_2 \rangle_{\text{tree}} \right\}, \quad (19)$$

where $C_F = 4/3$, $N = 3$ is the number of colors, and $\langle Q_i \rangle_{\text{tree}}$ is the tree level matrix elements of the operators.

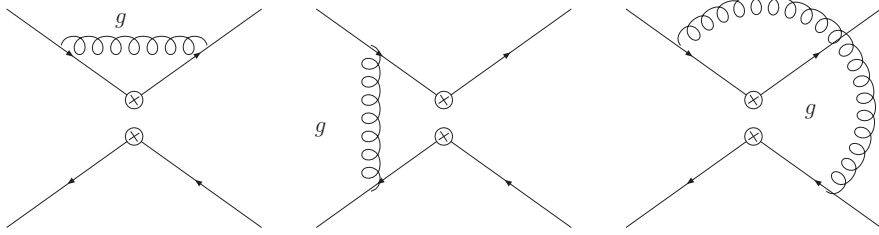


FIG. 2: The next-to-leading-order corrections in the effective theory.

In the effective theory, there are remaining UV divergences after taking into account the quark field renormalization, which must be canceled by the renormalization of the effective operators. Calculating the diagrams in Fig. 2 with the insertion of the operators Q_1 and Q_2 , we get the following amplitudes after quark field renormalization:

$$\langle Q_1^0 \rangle = \left[1 + \frac{\alpha_s}{2\pi} C_F \left(\frac{3}{\hat{\epsilon}} + 2 - 4 \ln \frac{m_Q^2}{\mu^2} \right) + \frac{\alpha_s}{4\pi} \ln \frac{m_Q^2}{m_q^2} \right] \langle Q_1 \rangle_{\text{tree}} - \frac{\alpha_s}{4\pi} \frac{1}{N} \ln \frac{m_Q^2}{m_q^2} \langle Q_2 \rangle_{\text{tree}}, \quad (20)$$

$$\begin{aligned} \langle Q_2^0 \rangle &= \frac{\alpha_s}{4\pi} \left(\frac{3}{\hat{\epsilon}} + 1 - 3 \ln \frac{m_Q^2}{\mu^2} - \frac{1}{N} \ln \frac{m_Q^2}{m_q^2} \right) \langle Q_1 \rangle_{\text{tree}} \\ &+ \left[1 - \frac{\alpha_s}{4\pi} \frac{1}{N} \left(\frac{3}{\hat{\epsilon}} + 1 - 3 \ln \frac{m_Q^2}{\mu^2} \right) + \frac{\alpha_s}{2\pi} C_F \left(1 - \ln \frac{m_Q^2}{\mu^2} \right) + \frac{\alpha_s}{4\pi} \ln \frac{m_Q^2}{m_q^2} \right] \langle Q_2 \rangle_{\text{tree}}, \end{aligned} \quad (21)$$

where $1/\hat{\epsilon} = 1/\epsilon - \gamma_E + \ln 4\pi$. The renormalization constant matrix for the two operators is

$$\hat{Z}_Q = 1 + \frac{\alpha_s}{4\pi} \frac{1}{\hat{\epsilon}} \begin{pmatrix} 8 & 0 \\ 3 & -1 \end{pmatrix}, \quad (22)$$

from which we obtain the anomalous dimension matrix:

$$\hat{\gamma}_Q = -\frac{\alpha_s}{2\pi} \begin{pmatrix} 8 & 0 \\ 3 & -1 \end{pmatrix}. \quad (23)$$

Our results of anomalous dimensions agree with those in Ref. [26].

Matching the results in the full theory and the effective theory, we extract the Wilson

coefficients:

$$C_1(m_{\tilde{\nu}}) = - \sum_i \frac{\lambda'_{ijk} \lambda'^*_{ikj}}{m_{\tilde{\nu}}^2} \left(1 + \frac{\alpha_s}{4\pi} \frac{x \ln x}{1-x} \right), \quad (24)$$

$$C_2(m_{\tilde{\nu}}) = \sum_i \frac{\lambda'_{ijk} \lambda'^*_{ikj}}{m_{\tilde{\nu}}^2} \frac{\alpha_s}{4\pi} \frac{1}{N} \frac{x \ln x}{1-x}, \quad (25)$$

where $x = m_Q^2/m_{\tilde{\nu}}^2$. These coefficients satisfy the renormalization group equations

$$\frac{d}{d \ln \mu} \begin{pmatrix} C_1(\mu) \\ C_2(\mu) \end{pmatrix} = \hat{\gamma}_Q^T(\alpha_s(\mu)) \begin{pmatrix} C_1(\mu) \\ C_2(\mu) \end{pmatrix}, \quad (26)$$

from which we can solve the Wilson coefficients for arbitrary scale μ .

Δm_B , $S_{J/\psi K_s(\phi)}$ are defined in terms of the matrix element $\langle \bar{B}_{s(d)} | \mathcal{H}_{eff}^{\Delta B=2} | B_{s(d)} \rangle$, which can be written as

$$\langle \bar{B}_{s(d)} | \mathcal{H}_{eff}^{\Delta B=2} | B_{s(d)} \rangle = \mathcal{A}_{SM} + \mathcal{A}_{RPV} = \mathcal{A}_{SM} \left(1 + \frac{\mathcal{A}_{RPV}}{\mathcal{A}_{SM}} \right), \quad (27)$$

where \mathcal{A}_{SM} and \mathcal{A}_{RPV} denote matrix elements of the SM and the MSSM-RPV effective hamiltonian, respectively. With the above matrix element, Δm_B and $S_{J/\psi K_s(\phi)}$ can be expressed

$$\begin{aligned} \Delta m_B &= 2 \left| \langle \bar{B}_{s(d)} | \mathcal{H}_{eff}^{\Delta B=2} | B_{s(d)} \rangle \right| = \Delta m_B^{SM} \left| 1 + \frac{\mathcal{A}_{RPV}}{\mathcal{A}_{SM}} \right|, \\ S_{J/\psi K_s(\phi)} &= \sin \left(2\beta_{(s)} + \arg \left(1 + \frac{\mathcal{A}_{RPV}}{\mathcal{A}_{SM}} \right) \right), \end{aligned} \quad (28)$$

where Δm_B^{SM} and $\beta_{(s)}$ denotes the SM contributions, respectively. In Eq.(28), hadronic uncertainties arising from hadron decay constants cancel between \mathcal{A}_{SM} and \mathcal{A}_{RPV} , and hadronic uncertainties remain only in Δm_B^{SM} and $\beta_{(s)}$. As for $K^0 - \bar{K}^0$ mixing, Δm_K can be obtained straightforwardly.

IV. NUMERICAL RESULTS

In this section we present our numerical results. The SUSY scale is taken to be the mass of the sneutrino $m_{\tilde{\nu}}$. The CKM matrix elements are parametrized in the Wolfenstein convention with four parameters $A = 0.809$, $\lambda = 0.2272$, $\rho = 0.197$ and $\eta = 0.339$. The other standard model parameters are taken to be $G_F = 1.16637^{-5} \text{ GeV}^{-2}$, $\alpha_s(m_Z) = 0.118$, $m_t =$

173 GeV [27]. The mass of B meson and K meson are $m_{B_s} = 5367.5$ MeV, $m_{B_0} = 5279.4$ MeV and $m_K = 497.648$ MeV [27]. The time-dependent CP asymmetry in B_d decay $S_{J/\psi K_s} = 0.687^{+0.032}_{-0.032}$ [27]. The recent experimental values of the mass differences of the B_d and K^0 mesons mixing are $\Delta m_K = (0.5292 \pm 0.0009) \times 10^{-2} \text{ ps}^{-1}$, $\Delta m_{B_d} = 0.507^{+0.005}_{-0.005} \text{ ps}^{-1}$ [27], and Δm_s is shown in Eq. (1).

In our numerical calculations, we first neglect the uncertainties from the hadronic parameters in the SM and assume that the predictions of the SM can reproduce the central values of the experimental data. Thus we demand that the RPV contributions must not exceed the experimental upper and lower bounds of the corresponding data.

First, we consider the new measurement of $B_s - \bar{B}_s$ mixing, which can constrain the combination $\Lambda_{32} \equiv \sum_i \lambda'_{i32} \lambda'^*_{i23}$ once the sneutrino mass is given. Fig. 3 shows the allowed region in the $\Lambda_{32} - m_{\tilde{\nu}}$ plane, where the gray area and the dark area is the allowed region extracted from the leading-order amplitude. We find that with the new data, the couplings are constrained to the level of 10^{-9} . After including the NLO QCD corrections, the gray area is excluded and only the dark area survives. One can see that since the NLO QCD effects increase the resulting mass difference, the bound is more stringent (about 50% lower) than that from LO calculations. If setting $m_{\tilde{\nu}} = 100$ GeV, the bounds on Λ_{32} from the calculations of LO and NLO are

$$\Lambda_{32} < 4.6 \times 10^{-9}(\text{LO}), \quad 2.4 \times 10^{-9}(\text{NLO}), \quad (29)$$

respectively.

Fig. 4 and Fig. 5 show the constraints on the combination $\Lambda_{31} \equiv \sum_i \lambda'_{i31} \lambda'^*_{i13}$ from $B_0 - \bar{B}_0$ mixing and $\Lambda_{21} \equiv \sum_i \lambda'_{i21} \lambda'^*_{i12}$ from $K_0 - \bar{K}_0$ mixing. The situation here is similar to that in $B_s - \bar{B}_s$ mixing: the NLO QCD corrections increase the mass differences and thus give more strong constraints on the combinations of couplings of MSSM-RPV. At the reference point $m_{\tilde{\nu}} = 100$ GeV, the bounds are

$$\Lambda_{31} < 2.9 \times 10^{-10}(\text{LO}), \quad 1.5 \times 10^{-10}(\text{NLO}), \quad (30)$$

$$\Lambda_{21} < 8.8 \times 10^{-14}(\text{LO}), \quad 2.8 \times 10^{-14}(\text{NLO}). \quad (31)$$

Above bounds are two and four orders of magnitude stronger than ones given in Ref. [16], as shown in Eq. (3), which is due to the fact that the updated data of the measurements and the contributions from the SM have been considered in our calculations.

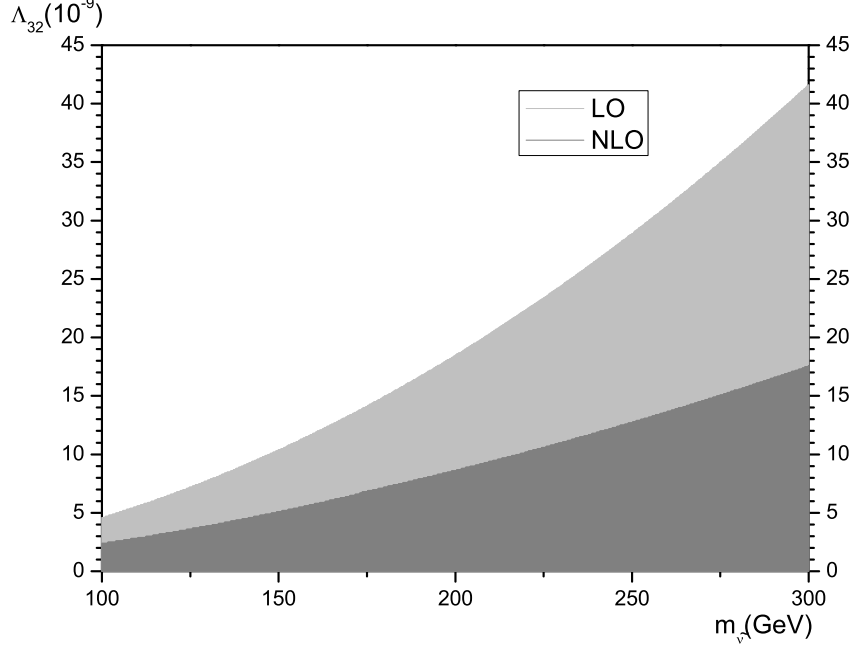


FIG. 3: The bounds for $\sum_i \lambda'_{i32} \lambda'^*_{i23}$ vary with the mass of the sneutrino. The gray area and the dark area are the allow region extracted from the LO amplitude. After NLO corrections, the gray area is excluded and only the dark area survives.

We further consider the situation that the hadronic uncertainties are involved. In this case, the bounds on the combinations of couplings in MSSM-RPV are looser than those in Eqs. (29), (30) and (31). The new bounds from the three observables are

$$\begin{aligned}
\Lambda_{32} &< 12.392 \times 10^{-8} \quad (\text{LO}), \\
&< 6.481 \times 10^{-8} \quad (\text{NLO}); \\
\Lambda_{31} &< 7.833 \times 10^{-9} \quad (\text{LO}), \\
&< 4.096 \times 10^{-9} \quad (\text{NLO}); \\
\Lambda_{21} &< 3.47 \times 10^{-11} \quad (\text{LO}), \\
&< 1.39 \times 10^{-11} \quad (\text{NLO}),
\end{aligned} \tag{32}$$

respectively.

We also discuss the situation that Λ_{ij} is complex, and parametrize the combinations of relevant couplings as $\Lambda_{ij} = |\Lambda_{ij}| e^{2i\sigma_{ij}}$, where ij can be 32 and 31. After assuming arbitrary

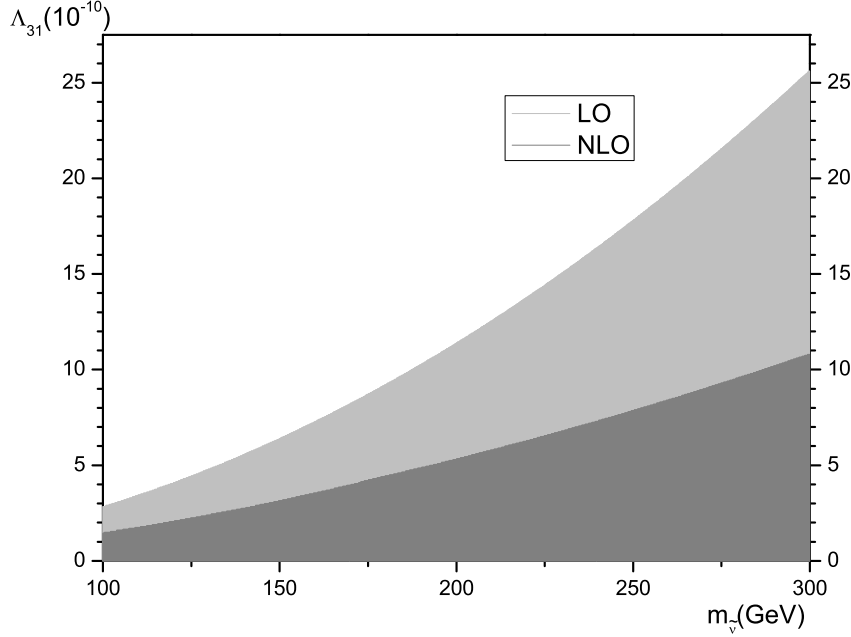


FIG. 4: The bounds for $\sum_i \lambda'_{i31} \lambda_{i13}^*$ vary with the mass of the sneutrino.

phases σ_{ij} , we can obtain constraints on the magnitude $|\Lambda_{ij}|$. Fig. 6 and Fig. 7 shows the allowed range of Λ_{32} and Λ_{31} for $m_{\tilde{\nu}} = 100\text{GeV}$, taking into account the constraints from Δm_s and Δm_d . For the $B_s - \bar{B}_s$ mixing, Λ_{32} is about $\mathcal{O}(10^{-9})$, while for the $B_d - \bar{B}_d$ mixing, Λ_{31} is about $\mathcal{O}(10^{-11})$. In both figures, there are additional areas with large $|\Lambda_{ij}|$ besides ordinary areas with small $|\Lambda_{ij}|$, which correspond to ones where contributions from the MSSM-RPV are larger than those from the SM, roughly twice the SM contributions but with different signs. We do not discuss complex couplings in K system due to the fact that Eq. (13) holds only under the condition that imaginary part of $\langle \bar{K}^0 | \mathcal{H}_{\text{eff}} | K^0 \rangle$ is far less than the real part.

The combinations of complex couplings can introduce new CP-violation origins, so we further investigate how the CP asymmetries in B decays constrain these combinations of couplings. Using the experimental data of $S_{J/\psi K_s}$ [27], we plot the allowed areas of the magnitude $|\Lambda_{31}|$ and the phase σ_{31} in Fig.8, which shows that the upper bound for $|\Lambda_{31}|$ is generally about $\mathcal{O}(10^{-10})$, except for some special values of σ_{31} . Those special values correspond to $\arg(1 + \mathcal{A}_{RPV}/\mathcal{A}_{SM}) = 0$, and we have $\sin(2\beta_{\text{eff}}) = \sin(2\beta)$. In fact, another

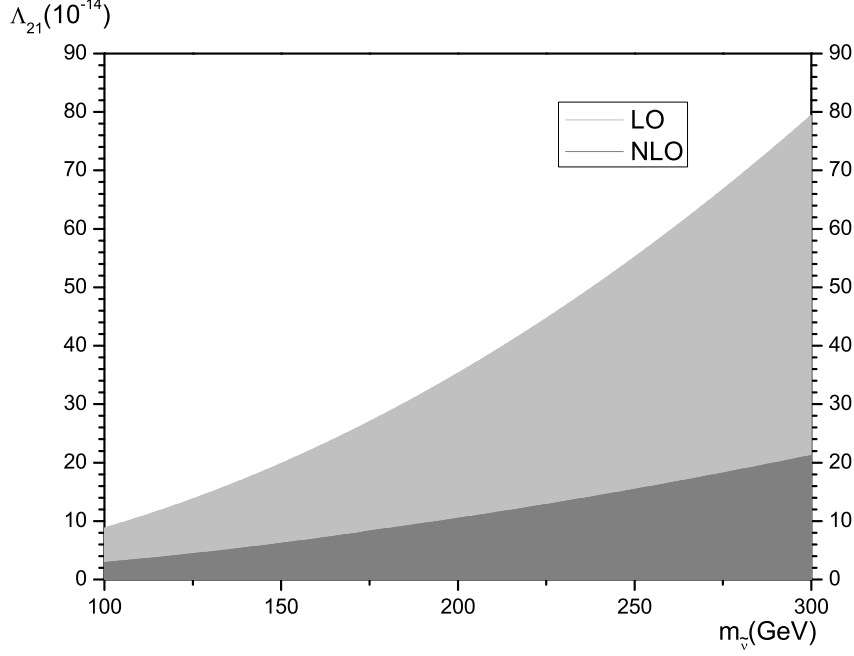


FIG. 5: The bounds for $\sum_i \lambda'_{i21} \lambda_{i12}^*$ vary with the mass of the sneutrino.

area with $\arg(1 + \mathcal{A}_{RPV}/\mathcal{A}_{SM}) = \pi - 4\beta$ also survives from constraint of experiment data of $S_{J/\psi K_s}$, however, this possibility has been excluded by an angular analysis of $B^0 \rightarrow J/\psi K^{*0}$ and a time-dependent Dalitz plot analysis of $B^0 \rightarrow \bar{D}^0 h^0 (h^0 = \pi^0, \eta^0, \omega)$ [28]. For the CP asymmetry in B_s decays, although there is no experimental data of $S_{J/\psi\phi}$ currently, future LHCb experiment will provide enough data to reach $\sigma_{stat}(S_{J/\psi\phi}) \approx 0.03$ in the first year [29], which would provide a strong constraint on new physics. So we assume $S_{J/\psi\phi} = 0.04 \pm 0.03$ and plot constraints on $|\Lambda_{32}|$ and σ_{32} in Fig.9, which shows that the upper bound for $|\Lambda_{32}|$ is about $\mathcal{O}(10^{-8})$ except for some special values of σ_{32} similar to the case of $S_{J/\psi K_s}$.

In conclusion, using the updated data, we have calculated contributions to $B_s - \bar{B}_s$ mixing, $B_d - \bar{B}_d$ mixing and $K^0 - \bar{K}^0$ mixing in the framework of the minimal supersymmetric standard model with R-parity violation including NLO QCD corrections, and presented new constraints on the relevant couplings of MSSM-RPV. Our results show that upper bound on the relevant combination of couplings of $B_s - \bar{B}_s$ mixing is of the order 10^{-9} , and upper bounds on the relevant combinations of couplings of $B_d - \bar{B}_d$ mixing and $K^0 - \bar{K}^0$ mixing are two and four orders of magnitude stronger than ones reported in Ref. [16], respectively. We

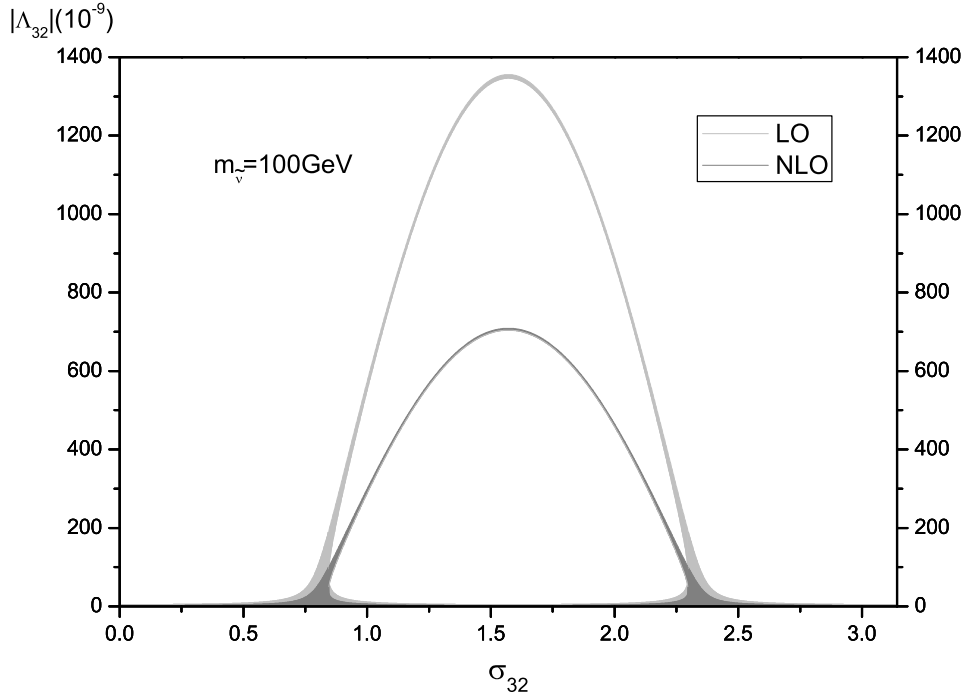


FIG. 6: The allowed range of the magnitude and phase of $\sum_i \lambda'_{i32} \lambda_{i23}^*$ constrained by the updated experimental data of Δm_s . The gray area accounts for the tree level results. When the QCD corrections are added, the allowed area is reduced to the dark area.

also discussed the case of complex couplings and showed that how the relevant combinations of couplings are constrained by the updated experiment data of $B_s - \bar{B}_s$, $B_d - \bar{B}_d$ mixing and time-dependent CP asymmetry $S_{J/\psi K_s}$, and future possible observations of $S_{J/\psi \phi}$ at LHCb, respectively.

Note added. While preparing this manuscript the paper of [30] appeared where the same coupling combination from $B_s - \bar{B}_s$ mixing is also discussed. However, the authors of [30] mainly dealt with contributions through the box diagram. Our results induced by the tree-level diagram is a few orders of magnitude stronger than theirs.

Acknowledgments

This work was supported in part by the National Natural Science Foundation of China, under Grant No. 10421503, No. 10575001 and No. 10635030, and the Key Grant Project of

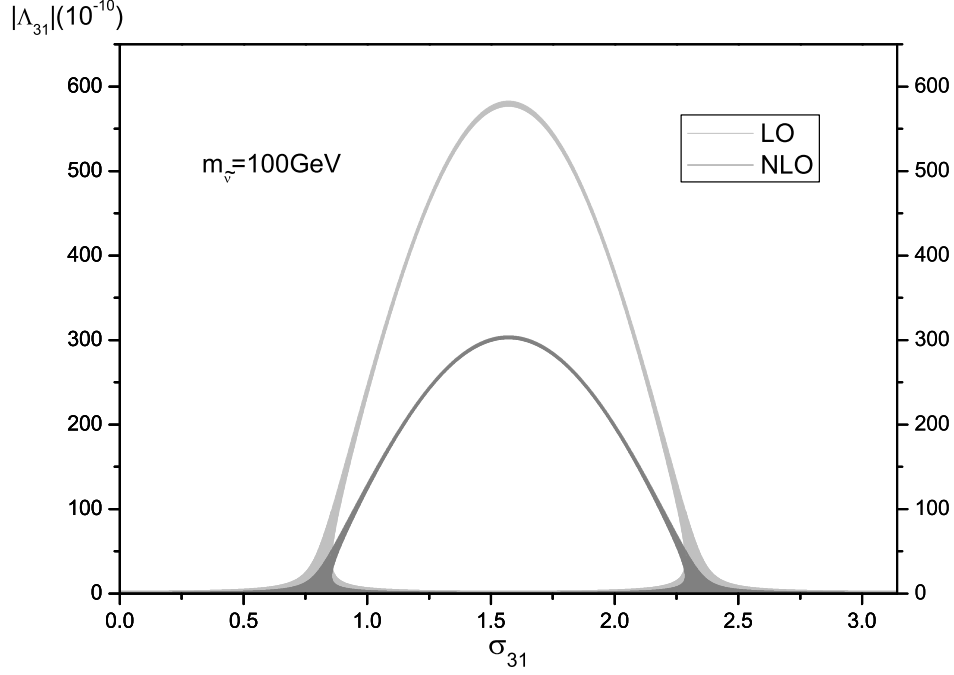


FIG. 7: The allowed range of the magnitude and phase of $\sum_i \lambda'_{i31} \lambda'^*_{i13}$ constrained by the experimental data of Δm_d .

Chinese Ministry of Education under Grant No. 305001 and the Specialized Research Fund for the Doctoral Program of Higher Education.

-
- [1] V. Abazov *et al.* (D0 Collaboration), Phys. Rev. Lett. 97, 021802 (2006).
 - [2] A. Abulencia *et al.* (CDF collaboration), Phys. Rev. Lett. 97, 062003 (2006); hep-ex/0609040.
 - [3] Monika Blanke, Andrzej J. Buras, Diego Guadagnoli, Cecilia Tarantino, hep-ph/0604057.
 - [4] Z. Ligeti, M. Papucci and G. Perez, Phys. Rev. Lett. 97 101801 (2006).
 - [5] P. Ball and R. Fleischer, hep-ph/0604249.
 - [6] Alakabha Datta, Phys. Rev. D74 (2006) 014022.
 - [7] UTfit Collaboration: M. Bona, *et al.*, Phys. Rev. Lett. 97, 151803 (2006).
 - [8] M. Ciuchini, L. Silvestrini, Phys. Rev. Lett. 97 (2006) 021803.
 - [9] M. Blanke, A. J. Buras, A. Poschenrieder, C. Tarantino, S. Uhlig, A. Weiler, hep-ph/0605214.

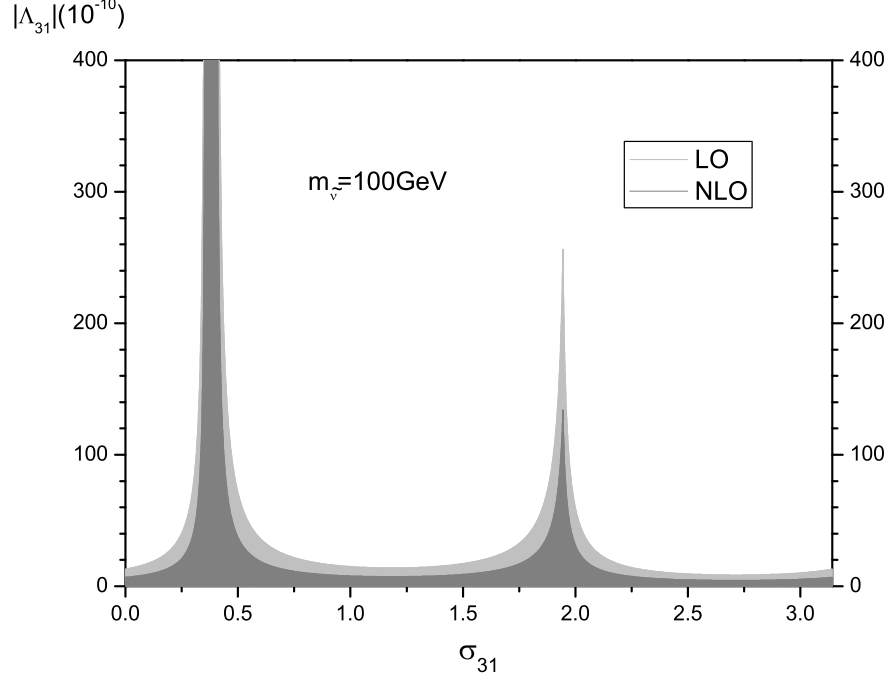


FIG. 8: The allowed range of the magnitude and phase of $\sum_i \lambda'_{i31} \lambda'^*_{i13}$ using experimental data of $S_{J/\psi K_s}$.

- [10] Seungwon Baek, Jong Hun Jeon, C. S. Kim, hep-ph/0607113.
- [11] Kingman Cheung, Cheng-Wei Chiang, N. G. Deshpande, J. Jiang, hep-ph/0604223.
- [12] Bhaskar Dutta, Yukihiro Mimura, hep-ph/0607147.
- [13] Gino Isidori, Paride Paradisi, Phys. Lett. B639 (2006) 499-507.
- [14] J. K. Parry, hep-ph/0606150; hep-ph/0608192.
- [15] G. Farrar, P. Fayet, Phys. Lett. B 76 (1978) 575; R. Barbier, *et al*, Phys. Rept. 420 (2005) 1-202.
- [16] D. Choudhury, P. Roy, Phys. Lett.B 378 (1996) 153-158.
- [17] [Heavy Flavor Averaging Group (HFAG)], hep-ex/0603003.
- [18] Andrzej J. Buras, hep-ph/9806471.
- [19] F. J. Gilman, M. B. Wise, Phys. Rev. D 27 1128(1983).
- [20] A. J. Buras, M. Jamin, P. H. Weisz, Nucl. Phys. B347, 491 (1990); J. Urban, F. Krauss, U. Jentschura and G. Soff, Nucl. Phys. B523, 40(1998).

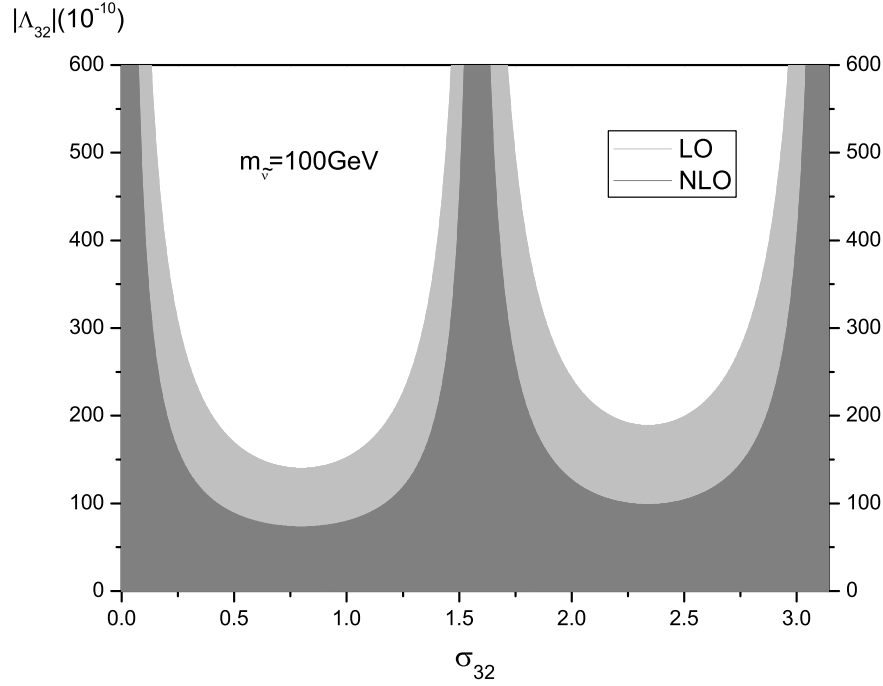


FIG. 9: The allowed range of the magnitude and phase of $\sum_i \lambda'_{i32} \lambda'^*_{i23}$, assuming the first year LHCb data provide an experiment measurement $S_{J/\psi\phi} = 0.04 \pm 0.03$.

- [21] T. Inami and C. S. Lim, Prog. Theor. Phys. 65, 297 (1981); 65, 1772(E) (1981).
- [22] S. Herrlich and U. Nierste, Nucl. Phys. B419, 292(1994); Phys. Rev. D52, 6505(1995) ; Nucl. Phys. B476, 27(1996).
- [23] G. C. Branco, L. Lavoura, J. P. Silva, CP Violation, Claredon Press · Oxford, 1999.
- [24] C. R. Allton, L. Conti, A. Donini, V. Gimenez, L. Giusti, G. Martinelli, M. Talevi, A. Vladikas, Phys. Lett. B453 (1999) 30-39.
- [25] D. Becirevic *et al.*, Nucl. Phys. B634, 105 (2002); D. Becirevic, V. Gimenez, G. Martinelli, M. Papinutto, and J. Reyes, JHEP. 04, 025 (2002); Nucl. Phys. B (Proc. Suppl.) 106. 385 (2002).
- [26] M. Ciuchini, E. Franco, V. Lubicz, G. Martinelli, I. Schimemi, L. Silvestrini, Nucl. Phys. B523 (1998) 501-525.
- [27] W.-M. Yao, *et al.*, (Particle Data Group), Review of Particle Physics, J. Phys. G: Nucl. Part. Phys. 33 (2006) 1.
- [28] B. Aubert *et al.*, [BABAR collaboration], Phys. Rev. D71, 032005 (2005); R. Itoh *et al.*,

- [Belle colabration], Phys. Rev. Lett. 95, 091601 (2005); K Abe *et al.*, [Belle colabration], hep-ex/0507065; For a comprehensive review, see Robert Fleischer, hep-ph/0608010.
- [29] O. Schneider, talk given at the Workshop on “Flavour in the era of LHC” First meeting, CERN, 2005, <http://lhcb-doc.web.cern.ch/lhcb-doc/presentations/conferencetalks/postscript/2005presentations/Schneider-epfl.pdf>.
- [30] S. Nandi, J. P. Saha, hep-ph/0608341